Reprint from The Review of DIABETIC STUDIES Vol 6 No 2 2009

The Review of DIABETIC STUDIES

ORIGINAL DATA

Allelic Variation of *Ets1* Does Not Contribute to NK and NKT Cell Deficiencies in Type 1 Diabetes Susceptible NOD Mice

Margaret A. Jordan[1], Lynn D. Poulton[2], Julie M. Fletcher[1] and Alan G. Baxter[1]

[1] *Comparative Genomics Centre, Molecular Sciences Bldg 21, James Cook University, Townsville, QLD 4811, Australia.*
[2] *Sir William Dunn School of Pathology, University of Oxford, South Parks Road, Oxford, OX1 3RE, United Kingdom.*
Address correspondence to: Alan G. Baxter, e-mail: alan.baxter@jcu.edu.au

Manuscript submitted July 24, 2009; resubmitted August 4, 2009; accepted August 8, 2009

■ Abstract

The NOD mouse strain is a well characterized model of type 1 diabetes that shares several of the characteristics of *Ets1*-deficient targeted mutant mice, viz: defects in TCR allelic exclusion, susceptibility to a lupus like disease characterized by IgM and IgG autoantibodies and immune complex-mediated glomerulonephritis, and deficiencies of NK and NKT cells. Here, we sought evidence for allelic variation of *Ets1* in mice contributing to the NK and NKT cell phenotypes of the NOD strain. ETS1 expression in NK and NKT cells was reduced in NOD mice, compared to C57BL/6 mice. Although NKT cells numbers were significantly correlated with ETS1 expression in both strains, NKT cell numbers were not linked to the *Ets1* gene in a first backcross from NOD to C57BL/6 mice. These results indicate that allelic variation of *Ets1* did not contribute to variation in NKT cell numbers in these mice. It remains possible that a third factor not linked to the *Ets1* locus controls both ETS1 expression and subsequently NK and NKT cell phenotypes.

Keywords: type 1 diabetes · NK cell · natural killer cell · NKT cell · NOD mouse · Ets1 · natural immunity · v-ets · erythroblastosis virus E26 oncogene

Introduction

The *v-ets* erythroblastosis virus E26 oncogene homolog 1 (previously E26 transformation-specific 1; *Ets1*) gene is located at position 32.5Mb (approximately 15cM) on mouse chromosome 9, and 128.3Mb on human chr11. ETS1 is a member of the Ets family of eukaryotic transcription factors [1], which play important roles in regulating gene expression, particularly of hemopoietic tissues, in response to multiple developmental and mitotic signals involved in stem cell development, proliferation, cell senescence and death, and tumorigenesis. The conserved ETS domain is a winged helix-turn-helix DNA-binding domain which recognizes the core consensus DNA sequence GGAA/T of target genes [2].

ETS1 is highly expressed in T, B and NK cells. It is first expressed in the thymus on e17-e18 of murine embryonic development, when mature single positive (SP) thymocytes begin to accumulate in large numbers. It is expressed at highest levels on $CD4^+CD8^-$ SP thymocytes and mature CD4 T cells [3]. Targeted deletion of *Ets1* resulted in significant fetal mortality and runting of live born mice [4]. In chimeric hemopoetic cell recipients, αβ-T cell development was impaired beyond the double negative ($CD4^-CD8^-$; DN) 3 ($CD44^-CD25^+$) stage and was associated with an elevated rate of cell death in the DN4 ($CD44^-CD25^-$) subset

and a reduction in the numbers of peripheral T cells to about 1/15th normal [5-7]. *Ets1* also appears to play an important role in TCR allelic exclusion, as the percentage of *Ets1*$^{-/-}$ thymocytes coexpressing two different TCR chains was increased, even in the presence of a TCRβ-expressing transgene [6]. Despite expressing normal levels of TCR and CD3, *Ets1*$^{-/-}$ T cells proliferated poorly in response to anti-CD3 ligation or ConA stimulation and had an approximately two times higher rate of spontaneous apoptosis *in vitro* than wild type T cells [5, 7].

Although peripheral B cell numbers were similar in RAG2$^{-/-}$ recipients reconstituted with *Ets1*$^{-/-}$ hemopoetic cells to those in chimeras reconstituted with wild type cells, they had almost no B-1a, transitional 2, and marginal zone B cells. Instead, they had a novel B220^{low}, IgM^{+}IgD^{-} population, a 10- to 15-fold expansion of plasmacytes, increased expression of activation markers on follicular B cells, and a 10-fold increase in serum IgM levels [7-9]. B cell survival was normal in chimeric mice reconstituted with *Ets1*$^{-/-}$ cells, although proliferative responses to anti-CD40 stimulation were halved [7]. Proliferation of B cells in response to LPS was reduced to about one third of normal [7, 8], consistent with a role for ETS1 in modulating *Tlr4* expression [10], but was increased in response to CpG DNA by more than two-fold [8]. Following BCR engagement with anti-IgM mAb, *Ets1*$^{-/-}$ B cells failed to proliferate, but instead underwent apoptosis [9].

Mice bearing targeted deletions of *Ets1* show severe defects in both NK and NKT cell numbers; numbers of DX5^{+}CD3^{-} cells in the spleen were approximately one third of wild type controls [4] and numbers of CD4^{+}NK1.1^{+} lymphocytes were markedly reduced in the thymus, spleen and liver of ETS1 deficient mice [11]. Since Walunas *et al.* (2000) used CD4 and NK1.1 as surrogate NKT cell markers in the absence of a specific NKT cell reagent, levels of Vα14Jα18 transcripts in the liver were compared between *Ets1*$^{-/-}$ mice and wild type controls. Vα14Jα18 transcripts were significantly decreased in ETS1-deficient mice and were present at similar levels to those found in NKT cell deficient *Cd1d*$^{-/-}$ mice, confirming that the reduction in CD4^{+}NK1.1^{-} lymphocytes reflected a reduction of type 1 NKT cells [11]. Additionally, no IL-4 was detected in the supernatants of *Ets1*$^{-/-}$ thymocytes stimulated with anti-CD3, consistent with an absence of thymic NKT cells [11]. The residual NK cells in ETS1-deficient mice were poorly cytolytic as they failed to kill either YAC-1 or MHC class I-deficient lymphoid blasts *in vitro*, or the NK cell-dependent MHC class I-deficient RMA-S tumor line *in vivo* [4]. The disproportionately poor lytic function of these cells may be related to the presence of an Ets-binding site motif capable of enhancing perforin expression in an NK cell-specific manner upstream of the *Prf1* gene [12].

ETS1 deficient mice appear to suffer a systemic autoimmune disease characterized by lymphadenopathy and mild infiltrates in liver and lungs and IgM and IgG autoantibodies with specificity against IgG, dsDNA, cardiolipin and myelin basement protein, leading to immune complex deposition in the kidneys [8].

The phenotype of *Ets1*$^{-/-}$ mice is reminiscent of several of the characteristics of the NOD mouse strain, a well characterized model of type 1 diabetes. For example, NOD mice are deficient in TCR allelic exclusion [13], are susceptible to a lupus like disease characterized by IgM and IgG autoantibodies and immune complex-mediated glomerulonephritis [14-19], and have deficiencies of NK [20] and NKT cells [21-24]. In addition to numerical deficiencies in peripheral NK and NKT cells, NOD mice exhibit functional defects in both populations. NK cells derived from NOD mice are poorly cytolytic, both *in vitro* and *in vivo*, compared to C57BL/6 NK cells, and NOD NKT cells are deficient in IL-4 production. There is considerable experimental evidence that NKT cell qualitative and quantitative defects are causally associated with the strain's susceptibility to type 1 diabetes. Increasing NKT cell numbers in NOD mice through a variety of experimental approaches such as adoptive transfer of αβTCR^{+}CD4^{-}CD8^{-} thymocytes enriched for NKT cells [21, 23], transgenic expression of the Vα14Jα18 TCR α-chain [25], or stimulation with the NKT cell super-antigen α-GalCer [26, 27] is associated with a decrease in the incidence of type 1 diabetes. Conversely, targeted deletion of the NKT cell restriction molecule, CD1d, which results in a complete absence of NKT cells, increases diabetes incidence in mice of the NOD genetic background [28, 29].

We therefore investigated the possibility that the deficiencies observed in NK and NKT cells in NOD mice are due to a defect or allelic difference in the expression of ETS1 in these cells or their precursors.

Materials and methods

Mice

NOD/Lt, BALB/c, C57BL/6 and NOD.*Nkrp1*^{b} [20] were obtained from the Animal Resources

Centre (ARC) (Canning Vale, WA, Australia). Specific experimental crosses, such as (NOD.*Nkrp1*^{b} × C57BL/6) × NOD.*Nkrp1*^{b}, were generated as needed in the animal facility of the Centenary Institute (Sydney, Australia) using mice purchased from the ARC. Mice were housed under specific pathogen-free conditions and all experiments were conducted with the approval of the Centenary Institute's animal ethics committee.

Cell suspension preparation

Cell suspensions from thymi were prepared by gently grinding the organ between two frosted microscope slides in FACS buffer (PBS/5% FCS). Cells were washed in 10 ml of FACS buffer and resuspended in 1 ml of FACS buffer until required. Spleens were disrupted using a 26-gauge needle and forceps and the resulting cell suspension was treated with red blood cell lysing buffer (Sigma, Castle Hill, NSW, Australia) for 7 min on ice. Livers were perfused *in situ* with 10 ml of cold PBS via the hepatic portal vein to avoid contamination with blood lymphocytes. The liver was cut into small pieces, pushed through a 200-guage steel mesh and the resulting suspension was washed twice in cold PBS. A 33.75% v/v isotonic Percoll density gradient (Amersham Biosciences, Sydney, NSW, Australia) was used to isolate hepatic lymphocytes. The resulting cell suspension was treated with red blood cell lysing buffer for 7 min on ice. Bone marrow cell suspensions were prepared by excising femurs and removing remaining muscle tissue. The ends of the femur were cut and the bone marrow was flushed from the shaft using a 26-gauge needle and syringe filled with PBS. The resulting cell suspension was treated with red blood cell lysing buffer for 7 min on ice. Blood samples, which were obtained by retro-orbital venipuncture, were centrifuged to remove plasma, and the resulting pellet was resuspended in red blood cell lysing buffer for 20 min on ice.

Flow cytometric analysis

Cells were pre-incubated with CD16/32 (clone 2.4G2, BD Biosciences, San Jose, CA, USA) to minimize non-specific staining due to FcR binding, before the addition of antibody cocktails. For surface staining, cells were incubated with αβTCR-FITC (clone H57-597), NK1.1-biotin (clone PK136) and CD49b-biotin (clone DX5) all from BD Biosciences. Biotinylated antibodies were detected using Streptavidin conjugated to PerCP (BD Biosciences). Mouse CD1d tetramer, conjugated to PE and loaded with α-Galactosylceramide was kindly provided by Professor Godfrey's laboratory (University of Melbourne, Australia). Viable lymphocytes were identified by the forward and side scatter profile. For intracellular ETS1 staining, cells were stained for surface markers, fixed in 4% formaldehyde, permeabilized in PBS/5%FCS/0.5% saponin and incubated with anti-ETS1 (clone sc-350; Santa Cruz Biotechnology, Santa Cruz, CA, USA). ETS1 antibody binding was detected with polyclonal anti-rabbit IgG conjugated to Texas Red (Southern Biotechnology, Birmingham, AL, USA). Flow cytometry was performed either on a FACscan or a FACstar plus flow cytometer (BD Biosciences) and data was analyzed using CellQuest software (BD Biosciences).

Protein Extraction and Western Blotting

Thymi were removed from 5 week-old female NOD/Lt, BALB/c and C57BL/6 mice. They were weighed and diced into small pieces using a clean razor blade and left in 3 ml ice cold RIPA buffer (50 mM Tris, pH 7.5, 150 mM NaCl, 1% Triton X-100, 1% Na-Deoxycholate, 0.1% SDS) per gram of tissue on ice for 30 minutes. Tissues were then homogenized with a Dounce homogenizer at 4°C, transferred to microfuge tubes, and incubated for a further 30 min on ice, followed by centrifugation at 10,000 g for 10 min at 4°C. The supernatant was removed and re-centrifuged as before. Supernatants were recovered and stored at -80°C prior to analysis. 50 µg whole cell lysate, with an equal volume of RIPA buffer and 10 µl loading buffer, was boiled for 5 min at 99°C. Samples were centrifuged at top speed for 4 min, before being loaded on a 15% SDS PAGE gel. Proteins were electrophoresed for 1 h at 40 mA on mini-PROTEAN 3 Cell (Bio-Rad, USA) and transferred from the gel to PDVF membrane in CAPS buffer (10 mM CAPS, 10% Methanol, pH 11). Non-specific binding was blocked by incubating the membrane in 1 × TBST (10 mM Tris-HCl, pH 8.0, 150 mM NaCl, 0.05% Tween20; 1% BSA), on ice overnight. The blocked membrane was incubated with anti-ETS1 (C20) antibody (clone sc-350, Santa Cruz Biotechnology) diluted in 1 × TBST; 0.1% BSA (1:20000), for 30 min at room temperature (RT). The membrane was washed 3 × 5 min in 1 × TBST (RT) followed by incubation with anti-rabbit antibody conjugated to alkaline phosphatase for 30 min at RT and then washed as before. Membranes were developed in 10 ml AP buffer containing 33 µl BCIP and 66 µl NBT (Santa Cruz Technology).

Table 1. Comparison of NK (NK1.1$^+$ αβTCR$^-$) and NKT (αGC/CD1d Tetramer$^+$ αβTCR$^+$) cell proportions and numbers between six week old female C57BL/6 (n = 5) and NOD.*Nkrp1*^{b} (n = 5) mice.

Organ	Strain	% NKT cells	# NKT cells (x 10^5)	% NK cells	# NK cells (x 10^5)
Thymus	C57BL/6	0.65 ± 0.05*	13.0 ± 0.6*	ND	ND
	NOD.*Nkrp1*^{b}	0.22 ± 0.02	3.5 ± 0.3	ND	ND
Spleen	C57BL/6	0.85 ± 0.01*	6.0 ± 1.0*	3.5 ± 0.61*	23.7 ± 2.5*
	NOD.*Nkrp1*^{b}	0.56 ± 0.04	3.0 ± 0.3	2.4 ± 0.2	14.5 ± 0.5
Liver	C57BL/6	16.8 ± 1.8*	3.5 ± 0.7*	8.8 ± 1.5	0.7 ± 0.2
	NOD.*Nkrp1*^{b}	9.2 ± 0.6	1.3 ± 0.2	7.8 ± 0.7	0.4 ± 0.1
Blood	C57BL/6	0.07 ± 0.0*	0.02 ± 0.002	7.9 ± 0.9*	1.9 ± 0.4*
	NOD.*Nkrp1*^{b}	0.13 ± 0.02	0.03 ± 0.004	4.3 ± 0.5	0.5 ± 0.1
Bone marrow	C57BL/6	0.51 ± 0.1*	1.1 ± 0.2*	1.6 ± 0.1*	2.6 ± 0.5*
	NOD.*Nkrp1*^{b}	0.14 ± 0.02	0.25 ± 0.04	2.5 ± 0.1	5.6 ± 0.2

Legend: ND = not determined. * indicates significant difference compared with NOD.*Nkrp1*^{b}, $p < 0.05$, Mann-Whitney U test.

RNA Preparation

Thymi were removed from 6 wk-old female mice directly into RNA-later (Qiagen, Hilden, Germany) and stored at -80°C until ready for extraction. The thymi were individually homogenized in the RLT buffer of an RNeasy kit (Qiagen), with contamination minimized by extensive washing with RNase-off and RNase-free-DNase-free-water between samples. Homogenates were passed through Qiashedder columns (Qiagen) and extracted (RNeasy, Qiagen). The RNA yield was quantified spectrophotometrically and aliquots electrophoresed for determination of sample concentration and purity.

Sequencing mRNA

As only the mRNA sequence was available, primers for sequencing were designed using Bio-Technix 3d 1.1.0, based on sequence obtained from NCBI (http://www.ncbi.nlm.nih.gov/sites/entrez) such that overlapping sequences would be amplified across the whole region. RNA was extracted from NOD/Lt, BALB/c and C57BL/6 mouse thymi and first-strand cDNA was synthesized from 5 µg total RNA using oligo(dT) primers and Superscript II reverse transcriptase following manufacturer's instructions (Invitrogen, Cambridge, UK). PCR was performed using Omn-E thermal cyclers (Hybaid, Basingstoke, UK). Each 100 µl reaction included 10 µl 10 × PCR buffer with 3 mM MgCl2 (Roche, Mannheim, Germany), 0.4 mM each of dATP, dCTP, dGTP and dTTP (Astral Scientific, Caringbah, NSW, Australia), 1.6 U Taq Polymerase (Roche), 2 µl cDNA. Approximately 20 µl mineral oil overlaid the reaction mix. PCR protocol included denaturation 95°C, 3 mins, then 40 cycles (95°C, 1 min; 50-62°C (primer dependant annealing) 1 min, 72°C, 1 min) followed by an extension step of 72°C, 7 min. Reactions were verified by 1% agarose gel electrophoresis. Reactions were then purified using the Qiagen PCR purification kit following manufacturer's directions. 20-100 ng PCR product between 200-500 bp/ 100-160 ng PCR product between 500-1000 bp were prepared with 6.4 pmol primer and sent to the Australian Genome Research Facility for sequencing (both forward and reverse reactions for each). The raw data was retrieved by FTP and analysed using Sequencher 3.1.1. (Gene Codes Corporation, Ann Arbor, Michigan, USA).

Sequencing genomic DNA

Inverse polymerase chain reaction (PCR) was used to obtain the unknown genomic sequence flanking the region of known sequence. This method uses the PCR, but it has the primers oriented in the reverse direction from the usual orientation. DNA was phenol-chloroform extracted from mouse tails, and used as a template for the reverse primers, following a restriction digest and ligation of the fragment upon itself to form a circle. The new sequences were then BLASTED using the CELERA Discovery System database (http://www.celera.com/) to look for contigs matching the known sequence. In this manner, we were able to obtain a number of overlapping contigs which could be assembled to give sequence 5' to

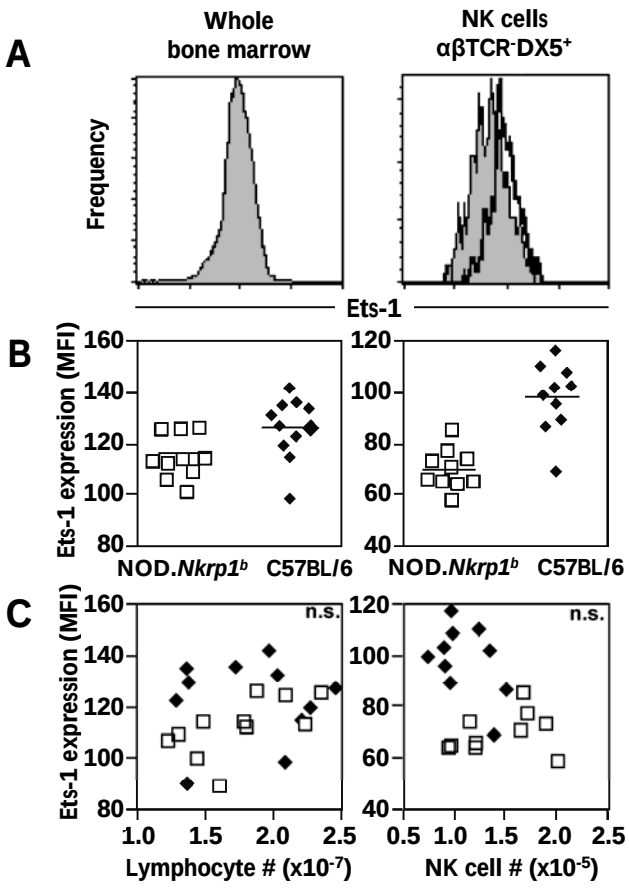

Figure 1. ETS1 expression in whole bone marrow (**A**, left) and bone marrow-derived NK (αβTCR$^-$DX5$^+$) cells (**A**, right) from three week old female NOD.*Nkrp1*^{b} (grey) and C57BL/6 (black line) mice, as determined by intracellular staining. **B**: Mean fluorescence intensity (MFI) of ETS1 staining in whole bone marrow (left) and bone marrow-derived NK cells (right) of individual NOD.*Nkrp1*^{b} and C57BL/6 mice. White squares: NOD.*Nkrp1*^{b}. Black diamonds: C57BL/6. **C**: Correlation of thymic NK ETS1 expression and thymic NK cells numbers. White squares: NOD.*Nkrp1*^{b}. Black diamonds: C57BL/6.

the start site as well as within intronic regions. Using the assembled sequence, primers were then designed such that overlapping sequences could be amplified for the different mouse stains. PCR and sequencing was carried out as before and the resulting sequence compared between strains using Sequencher 3.1.1. (Gene Codes Corporation, Ann Arbor, MI, USA).

Genotyping

Genotyping of the NOD.*Nkrp1*^{b}, C57BL/6, (NOD.*Nkrp1*^{b} × C57BL/6)F1 and (NOD.*Nkrp1*^{b} × C57BL/6) × NOD.*Nkrp1*^{b})BC1 mice was carried out by PCR of phenol-chloroform extracted tail DNA using primers designed across the SNP identified in Exon IV, followed by an *Nla*III restriction digest. PCR were performed on Omn-E thermal cyclers (Hybaid). Each 100 µl reaction included 10 µl 10x PCR buffer with 3 mM $MgCl_2$ (Roche), 0.4 mM each of dATP, dCTP, dGTP and dTTP (Astral), 1.6 U Taq Polymerase (Roche), 20 ng DNA. Approximately 20 µl mineral oil overlaid the reaction mix. PCR protocol included denaturation 95°C, 3 min, then 32 cycles (95°C, 1 min; 55°C, 1 min, 72°C, 1 min) followed by an extension step of 72°C, 7 min. Reactions were verified by 1% agarose gel electrophoresis. An analytical scale restriction digest was performed in 50 µl, using 20 µl PCR product, 5U *Nla*III, 0.05 µg Acetylated BSA, together with 5 µl RE 10x buffer. An incubation of 2 h at 37°C was carried out. Products were resolved on a 4% NuSieve gel. NOD alleles were identified as those that could be digested by *Nla*III, while C57BL/6 alleles remained undigested.

Typing of previously characterized microsatellite markers was performed as previously described [17, 30]. An additional microsatellite marker, *D9bax201* was designed in-house (by Dr. Luis Esteban) to determine the genotype of a locus within *Ets1*: forward primer TGGGGGCAG GAAGTATCTTTACAG, reverse primer TTCCTCCTCTCCTGAACAGATGAG.

Linkage analysis

Genotyping errors were identified manually as double recombinants or by the error-checking function of Mapmaker/EXP [31] and were reamplified. Recombination distances between markers were calculated from recombination frequencies using the Mapmaker/EXP program [31]. Interval analysis of linkage to the proportions of thymic NKT cells was conducted using a version of Mapmaker/QTL (quantitative trait locus) 2.0b that was ported to run on the Pentium 4 under Windows 2000 by M. Butler. The output of Mapmaker provides a log-likelihood ratio for any putative QTL located at an arbitrary point between the markers genotyped. The significance thresholds used were those suggested by Lander and Kruglyak (1995) for analyses of mouse backcrosses; viz logarithm of odds (LOD) ≥ 3.3 for the

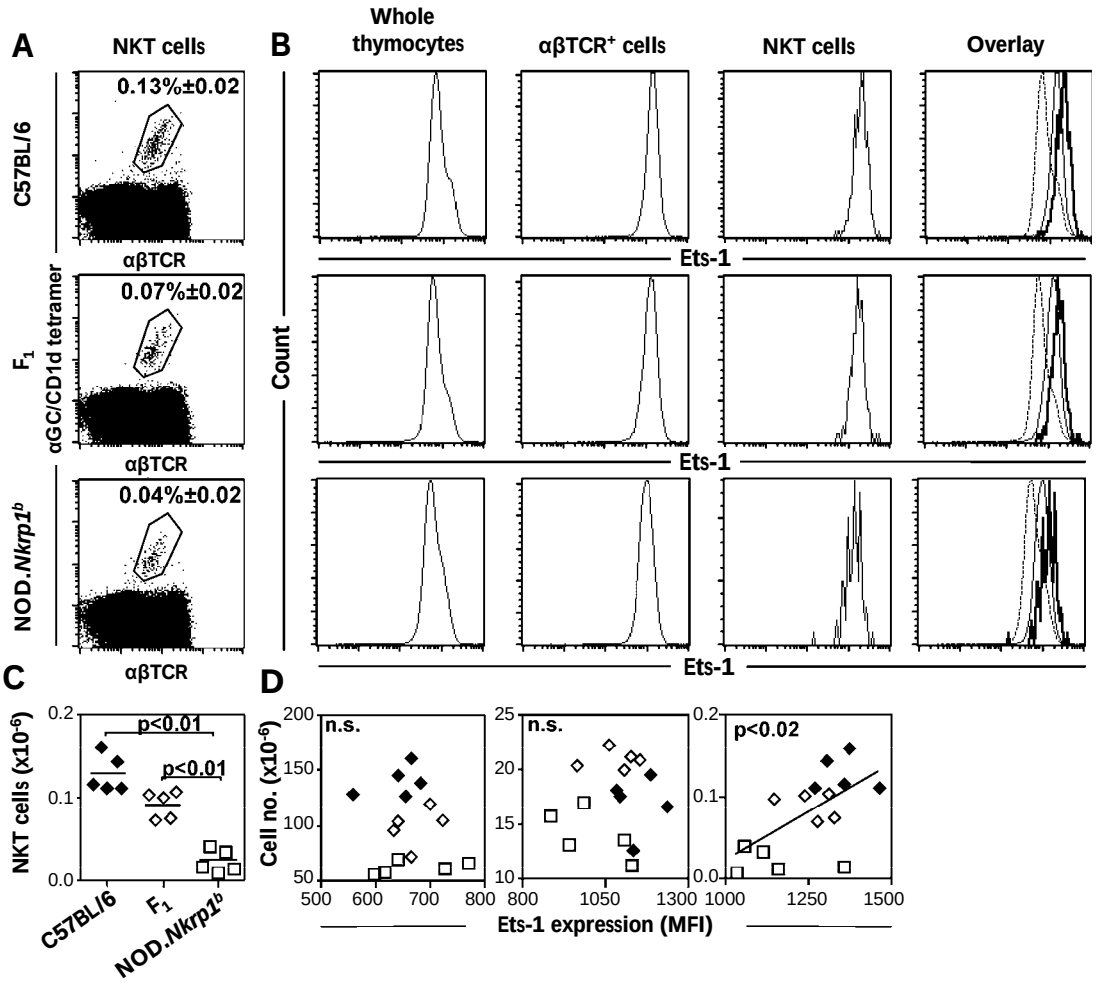

Figure 2. Representative FACS plots showing thymic NKT cell (αGC/CD1d Tetramer$^+$ αβTCR$^+$) proportions of three week old C57BL/6, NOD.*Nkrp1*^{b}, and (NOD.*Nkrp1*^{b} x C57BL/6)F1 mice (**A**). Mean proportions and standard errors are given for each. **B**: ETS1 expression in thymocytes (left), thymic T (αGC/CD1d Tetramer$^-$ αβTCR$^+$)(middle) and NKT (αGC/CD1d Tetramer$^+$ αβTCR$^+$) (right) cells from C57BL/6 (top panel), (NOD.*Nkrp1*^{b} × C57BL/6)F1 (middle panel) and NOD.*Nkrp1*^{b} (bottom panel) mice as determined by intracellular staining. Overlaid histograms (far right) depict ETS1 expression in whole thymocytes (dashed line), thymic T cells (thin line) and NKT cells (thick line) for C57BL/6, NOD.*Nkrp1b* and F1 mice. **C**: Absolute numbers of thymic NKT cells in C57BL/6 and F1 mice compared to NOD.*Nkrp1*^{b} mice ($p < 0.01$; Mann-Whitney U test). Black diamonds: C57BL/6. White diamonds: NOD.*Nkrp1*^{b} × C57BL/6)F1. White squares: NOD.*Nkrp1*^{b}. **D**: Correlation between NKT ETS1 expression and thymic NKT cell numbers (far right), total thymocyte numbers (left) and T cell numbers (middle). Black diamonds: C57BL/6. White diamonds: NOD.*Nkrp1*^{b} × C57BL/6)F1. White squares: NOD.*Nkrp1*^{b}.

threshold for significant linkage and LOD ≥ 1.9 for the threshold suggestive of linkage [32]. Quantitative differences between samples were compared using the Mann-Whitney U (rank sum) test.

Other statistical analyses

Quantitative two-way comparisons were performed by Mann-Whitney U test.

Results

ETS1 expression in NK and NKT cells

Consistent with previous reports [20, 24], NOD.*Nkrp1*^{b} mice had significantly decreased proportions and absolute numbers of NK cells in the spleen and blood compared to C57BL/6 mice, while proportions and numbers in the bone mar-

Table 2. Comparison of ETS1 expression levels in NOD.*Nkrp1*^{b}, C57BL/6 and (NOD.*Nkrp1*^{b} × C57BL/6)F1 thymocytes

Strain	ETS1 expression on whole thymocytes (MFI)	ETS1 expression on αβTCR$^+$ thymocytes (MFI)	ETS1 expression on NKT cells (MFI)
NOD.*Nkrp1*^{b}	668 ± 73	1002 ± 105	1136 ± 128*
F1	638 ± 48	1077 ± 74	1255 ± 74
C57BL/6	671 ± 37	1142 ± 66	1348 ± 74*

Legend: * indicates significant difference, $p < 0.05$, Mann-Whitney U test.

row were increased, suggesting a possible defect in the export of NK cells (Table 1, $p < 0.05$, Mann-Whitney U test). Similarly, proportions and numbers of NKT cells were decreased in NOD.*Nkrp1*^{b} mice in the thymus, spleen and liver (Table 1, $p < 0.05$, Mann-Whitney U test). Since both NOD mice and mice deficient in ETS1 exhibit numerical defects in NK and NKT cells, evidence was sought for an association between ETS1 expression levels and numbers of NK and NKT cells.

Whole bone marrow from three week-old NOD.*Nkrp1*^{b} and C57BL/6 mice was surface stained with anti-DX5 and anti-αβTCR antibodies, followed by intracellular staining for ETS1. NK cells (DX5$^+$αβTCR$^-$) from NOD.*Nkrp1*^{b} mice had significantly decreased expression of ETS1 compared to the NK cells of C57BL/6 mice (Figure 1, A and B, $p < 0.005$, Mann-Whitney U-test). The decrease was specific to NK cells since whole bone marrow from both strains expressed similar levels of ETS1 (Figure 1, A and B). However, there was no correlation between ETS1 expression and NK cell numbers in either strain (Figure 1C). It is therefore unlikely that the reduced ETS1 expression characteristic of NOD mice contributes to the NK cell phenotype of the strain.

Thymocytes from three week-old NOD.*Nkrp1*^{b}, C57BL/6 and (NOD.*Nkrp1*^{b} × C57BL6)F1 mice were stained with antibodies against αβTCR and ETS1 in conjunction with the NKT cell specific αGalCer loaded CD1d tetramer. In both strains and F1 mice expression levels of ETS1 were higher in both mature conventional T cells (αβTCR$^+$Tetramer$^-$) and NKT cells (αβTCR$^+$Tetramer$^+$) compared to whole thymocytes (Figure 2B, Table 2). While there was no significant variation of ETS1 expression in whole thymocytes or αβTCR$^+$ thymocytes between NOD.*Nkrp1*^{b}, C57BL/6 and F1 mice, it was significantly decreased in thymic NKT cells in NOD.*Nkrp1*^{b} mice (Table 2). ETS1 expression on NKT cells of (NOD.*Nkrp1*^{b} × C57BL6)F1 mice was intermediate between the parental strains. Numbers of conventional T cells did not correlate with ETS1 expression. However, NKT cell numbers were significantly correlated with ETS1 expression in both strains ($p < 0.02$), consistent with a role for allelic ETS1 expression in control of NKT cell numbers.

Ets1 Genomic and cDNA Sequence Comparison between the NOD/Lt, BALB/c and C57BL/6 strains

Having established that the NOD.*Nkrp1*^{b} mouse strain had reduced ETS1 expression in NKT cells and that this positively correlated with NKT cell numbers, we next sought to identify polymorphisms in the genomic and/or cDNA sequence of *Ets1*. To compare genomic sequences between the strains it was necessary to amplify DNA by inverse PCR as described in the 'Materials and methods' section since genomic sequence was unavailable. The sequences obtained were annotated and submitted to NCBI for public access: AY134615.1 (NOD/Lt exons III through IX and complete cds); AY134614 (NOD/Lt promoter and exon A); AY134613 (C57 exons III through IX and

Table 3. Single base pair and variable number of tandem repeat changes in C57BL/6 mice compared to NOD/Lt and BALB/c mice

Region	Single base pair	VNTR
5' region	7	3
Exon A	0	0
Intron 1a	5 (+1 in NOD)	1
Intron 1b	22	2
Exon III	0	0
Intron 2	12	2
Exon IV	1	0
Intron 3	6	0
Exon V	0	0
Intron 4	10	1
Exon VI	0	0
Intron 5	9	1
Exon VII	0	0
Intron 6	62 (+13 in BALB/c)	5
Exon VIII	0	0
Intron 7	6	1
Exon IX	0	0

Table 4. *Ets1* splice donor/acceptor sites

Exon number	Exon size (bp)	5' splice donor	3' splice acceptor	Intron size (bp)
A	82	CC GG/gtgagtggca	ttccttacag/AC ATG	29.907
III	120	AAA G/gtatactttt	tctcttctcag/AC CCC	1.265
IV	201	AAA G/gtaaatgtgt	tttcttacag/AG GAT	2.709
V	78	A TCA/gtaagtgctat(c)t	ctccttttctag/GC TAC	0.920
VI	249	C GTG/gtaggtcac(a)tt	ttacctccag/GT AAA	3.928
VII	261	A CAG/gtaggcaccc	gtgcttccag/GA AGT	14.917
VIII	119	GAT GAG/gtatgtaatg	tttattacag/GTG GCC	1.278
IX	213			

Legend: *Ets1* splice donor/acceptor sites are conserved between NOD/Lt, BALB/c and C57BL/6 mouse strains except a T to C substitution of the 5' splice donor of B6 in intron 4 and a C to A substitution of 5'splice donor of B6 in intron 5. NOD/Lt and BALB/c proved to have identical boundary sequences

complete cds); AY134612 (C57 promoter and exon A); AY134611 (BALB/c exons III through IX and complete cds) and AY134610 (BALB/c promoter and exon A).

As some rearrangements in the promoter sequence can affect the rate of initiation [33], while others can influence the site at which initiation occurs, approximately 2.6kb of sequence 5' of the first exon of *Ets1* was analyzed and compared between the three strains. *Ets1* has a TATA-less promoter that lacks CAAT sequences and has a high G-C content upstream of multiple initiation sites. Our data showed ten polymorphisms between the strains within the promoter sequence, all in the C57BL/6 strain compared to NOD and BALB mice (Table 3). These comprised seven single base pair changes and three VNTRs. Consensus recognition sites for several transcription factors that may regulate the mouse *Ets1* promoter include AP1, RAR, ETS1 and NFkB [34-36]. Processing of the promoter sequence using "Promoter Scan" (PROSCAN Version 1.7) [37] predicted many significant signals. The promoter region consists of ten consensus recognition sequences for the transcription factor SP1 (seven on the reverse strand and three on the forward strand), two AP1 consensus sequences and six AP2 recognition sequences (4 on the forward strand and 2 on the reverse strand). Three GCF consensus sequences are present. Other significant signals include one each of SDR-RS, SIF, CTF, NF1, CTF-NF-1, CP1, APRT-mouse-US, Early-SBQ1, (early SP1), JCV repeated sequence and UCE.2. However, none of the polymorphisms found here are located within any of the predicted recognition sites.

Comparison of intronic sequences between the three strains revealed 141 single base pair changes and 16 VNTR's in C57BL/6 mice when compared to the NOD and BALB/c strains (Table 3). NOD/Lt mice differed from C57BL/6 and BALB/c mice with only a single base pair change in the initial 2.5 kb sequence of intron1 examined while there were five single base pair changes and one variable number of tandem repeat (VNTR) in the C57BL/6 strain. The final 3 kb of intron 1 contained 22 single base pair polymorphisms in B6 and two VNTRs. This is of interest as previous studies [34] have suggested that the first intron of *Ets1* contains elements necessary for tissue specific expression. Intron 2 showed 12 single base pair polymorphisms and two VNTRs in the B6 strain. C57BL/6 showed six single base pair changes in intron 3, 10 single base pair polymorphisms and one VNTR in intron 4 and nine single base pair mutations and one VNTR in intron 5. Interestingly, sequencing the 14.917 kb intron 6 region showed polymorphisms in both C57BL/6 and BALB/c mice compared to the NOD/Lt strain. There were 62 single base pair polymorphisms in B6 and 13 in the BALB/c strain, while five VNTRs were present in B6. It is possible that these are within important enhancer sequences. Comparison of Intron 7 sequences revealed six single base pair mutations and one VNTR in B6.

A comparison of splice sites between strains were conserved except a T to C substitution of the 5' splice donor of B6 in intron 4 and a C to A substitution of 5' splice donor of B6 in intron 5 (Table 4). NOD/Lt and BALB/c proved to have identical boundary sequences. As both the full length and spliced mRNAs have been found for all strains, these polymorphisms do not appear to prevent the splicing process, but could perhaps alter its efficiency.

To obtain cDNA sequence, primers were designed using BioTechnix 3d 1.1.0, based on sequence obtained from NCBI (http://www.ncbi.nlm.nih.gov/sites/entrez) such that overlapping sequences would be amplified across the whole region. PCR were performed on RNA extracted from

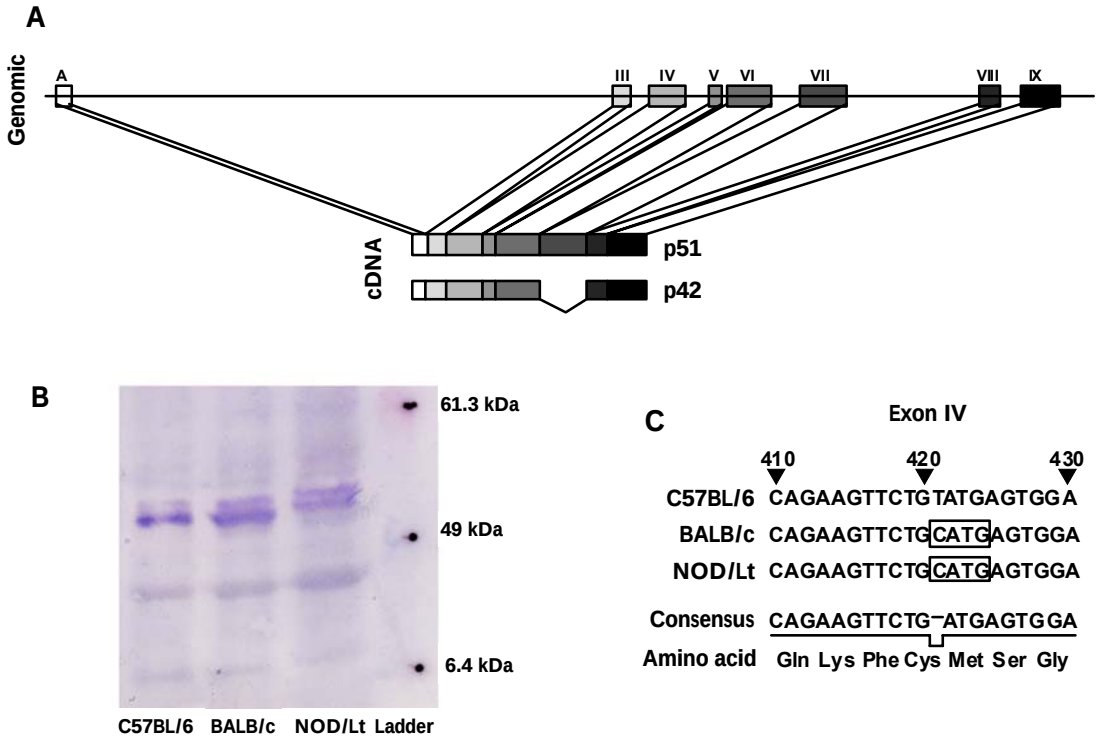

Figure 3. Schematic representation of the genomic structure of *Ets1* and cDNA for the p51 and p42 isoforms (**A**). **B**: Western blot analysis of 50 µg thymic whole cell lysates from five wk old female C57BL/6, BALB/c and NOD/Lt mice using anti-ETS1 mAb (clone sc-350) mapping to the carboxy terminus of ETS1. The mobility of BENCHMARK protein mass markers is indicated. **C**: Partial sequence of Exon IV (410-430 bp) showing a single T to C base pair change at position 421 that introduces the *Nla*III restriction enzyme site CATG (boxed).

NOD/Lt, BALB/c and C57BL/6 mouse thymi. Sequencing of the mRNA revealed two products identical between NOD/Lt, BALB/c and C57BL/6 except for a single base pair change at position 421 in both products which, although causing no change in the amino acid sequence, is an *Nla*III restriction site (Figure 3C). This restriction site was used for identifying allelic contribution in (NOD.*Nkrp1*^{b} × C57BL/6) × NOD.*Nkrp1*^{b} backcross (BC1) mice.

The full length mRNA produces the p51 isoform of the protein product and the spliced mRNA, which lacked exon VII, the p42 isoform (Figure 3A). Only these two isoforms were seen here, in contrast to the differential splicing noted in human *Ets1* studies which revealed sequences corresponding to the splicing out of exon IV, exon VII or both [38]. Western immuno-blotting of thymic protein extracts from NOD, BALB/c and C57BL/6 mice detected both ETS1 isoforms (Figure 3B). Consistent with previous reports [39, 40] the p51 isoform was present as a double band indicating the presence of the phosphorylated and non-phosphorylated protein, while the p42 isoform was present at a lower concentration.

Effects of the Ets1 allele on NKT cell numbers

To test the hypothesis that the observed allelic difference in ETS1 expression between NOD.*Nkrp1*^{b} and C57BL/6 mice was associated with reduced NKT cell numbers in NOD mice, seven week-old female (NOD.*Nkrp1*^{b} × C57Bl/6) × NOD.*Nkrp1*^{b} backcross (BC1) mice were assessed for thymic NKT cell numbers by flow cytometry. Thymic NKT cell phenotype was determined using an anti-αβTCR antibody in conjunction with NKT cell specific α-Galactosylceramide loaded CD1d tetramer. The BC1 mice were typed at the *Ets1* locus using *Nla*III restriction enzyme digest as described above. The proportions and numbers of thymic NKT cells were compared between BC1

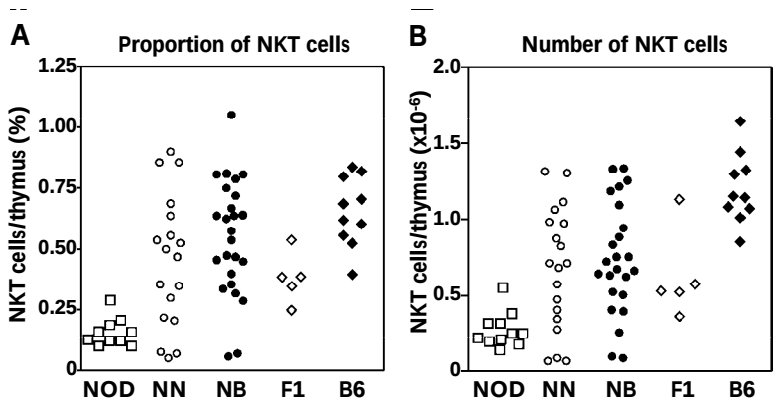

Figure 4. Proportion (**A**) and absolute number of thymic NKT (αβTCR$^+$ αGC/CD1d$^+$) cells (**B**) in seven week old female NOD.*Nkrp1*^{b} (NOD, open squares, n = 10), (NOD.*Nkrp1*^{b} x C56BL/6) × NOD.*Nkrp1*^{b} backcross mice either homozygous NOD (NN, open circles, n = 18) or heterozygous NOD/B6 (NB, black circles, n = 23) at the *Ets1* locus, (NOD.*Nkrp1*^{b} x C57BL/6)F1 (F1, white diamonds, n = 5) and C57BL/6 (B6, black diamonds, n = 10) mice.

mice homozygous NOD/NOD or heterozygous NOD/B6 at the *Ets1* locus. Consistent with previous results control C57BL/6 mice had increased proportions and absolute numbers of NKT cells in the thymus compared to NOD.*Nkrp1*^{b} mice, while numbers of NKT cells in control NOD.*Nkrp1*^{b} × C57BL/6 (F1) mice were intermediate between the parental strains (Figure 4, A and B). There was no significant difference in either proportions or numbers of thymic NKT cells between mice that were NOD/NOD or NOD/B6 at the *Ets1* locus (Figure 4, A and B).

In a second experiment, numbers of thymic NKT cells were determined by flow cytometric analysis of male (NOD.*Nkrp1*^{b} × C57BL/6) × NOD.*Nkrp1*^{b} BC1. The mice were phenotyped for thymic NKT cell numbers as described above and genotyped at the *Ets1* locus using *D9mit160, D9mit90, D9bax201, D9mit285, D9mit26, D9mit335, D9mit165, D9mit269, D9mit355, D9mit347 and D9mit17* microsatellite markers. Interval analysis of linkage to the proportions of thymic NKT cells was conducted using Mapmaker/QTL (quantitative trait locus) 2.0b with significance thresholds set at logarithm of odds (LOD) ≥ 3.3 for significant linkage and LOD ≥ 1.9 for suggestive linkage. No linkage of thymic NKT cell number to chromosome 9 was found (Figure 5).

The results of these two experiments show that there is a consistent difference in *Ets1* expression levels in NKT cells between the NOD.*Nkrp1*^{b} and C57BL/6 strains that is significantly correlated to NKT cell numbers. Despite this difference, the allelic variation of *Ets1* does not contribute to numerical NKT defects in the NOD strain.

Discussion

The complexity of the genetics of autoimmune traits has significantly impeded the fine localization and identification of disease susceptibility genes [41, 42]. We have attempted to overcome this problem by studying subphenotypes that contribute to the etiology of diabetes, and potentially many other autoimmune diseases, such as defects in immunoregulation [43]. Type 1 NKT cells are an immunoregulatory population that plays a critical role in controlling the strength and character of adaptive and innate immune responses [44]. Unlike conventional T cells, NKT cells can exhibit various natural killer (NK) cell characteristics, including ex-

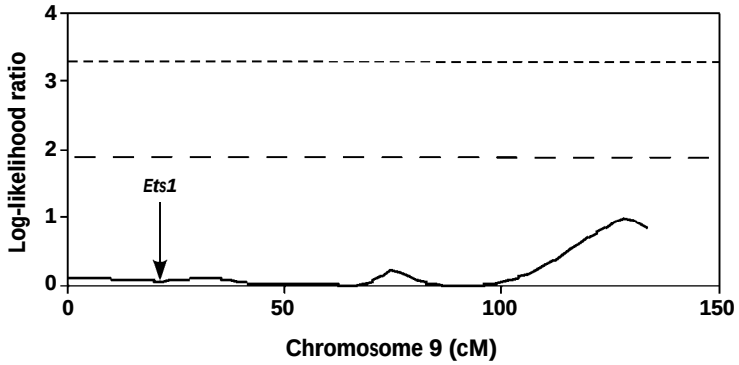

Figure 5. Linkage analysis for thymic NKT cell number on Chromosome 9 in (NOD.*Nkrp1*^{b} x C56BL/6) × NOD.*Nkrp1*^{b} backcross mice. The location of *Ets1* and the linkage thresholds set by Lander and Kruglyak [32] for significant linkage (LOD ≥ 3.3, short dashed line) and suggestive linkage (LOD ≥ 1.9, long dashed line) are shown.

pression of CD161c (NK1.1 in mice), and express a semi-invariant TCR consisting of an invariant Vα24-Jα18 (Vα14-Jα18 in mice) chain coupled to Vβ11 (Vβ2, 8.2 or 7 in mice) [45]. The NKT TCR recognises glycolipid, rather than peptide antigen, presented by the MHC Class I-like molecule CD1d [44].

We have previously reported deficiencies in the numbers and function of NKT cells in the NOD mouse strain [20-24], which is a well-validated model of type 1 diabetes and systemic lupus erythematosus [18, 46]. There is considerable experimental evidence that NKT cell qualitative and quantitative defects are causally associated with the strain's susceptibility to type 1 diabetes. Increasing NKT cell numbers in NOD mice through a variety of experimental approaches such as adoptive transfer of $\alpha\beta TCR^{+}CD4^{-}CD8^{-}$ thymocytes enriched for NKT cells [21, 23], transgenic expression of the Vα14Jα18 TCR α-chain [25], or stimulation with the NKT cell super-antigen α-GalCer [26, 27] is associated with a decrease in the incidence of type 1 diabetes. Conversely, targeted deletion of the NKT cell restriction molecule, CD1d, which results in a complete absence of NKT cells, increases diabetes incidence in mice of the NOD genetic background [28, 29].

Type 1 NKT cells are absent in mice bearing targeted deletions of *Ets1*. Barton *et al*. (1998) reported that numbers of $CD4^{+}NK1.1^{+}$ lymphocytes were markedly reduced in the thymus, spleen, and liver and that the levels of Vα14Jα18 transcripts in the liver were present at similar levels as NKT cell deficient $Cd1d^{-/-}$ [4]. Consistent with this finding, no IL-4 was detected in the supernatants of $Ets1^{-/-}$ thymocytes stimulated with anti-CD3 [11]. *Ets1* maps to the same chromosomal region of chromosome 9 as the NOD diabetes susceptibility gene *Idd2* [47, 48]. These findings raised the possibility that allelic variation in *Ets1* expression could affect the numbers of NKT cells, thereby affecting NKT cell numbers and susceptibility to diabetes.

ETS1 expression in NK and NKT cells was reduced in NOD.$Nkrp1^{b}$ mice, compared to C57BL/6 mice. Although NKT cells numbers were significantly correlated with ETS1 expression in both strains, NKT cell number was not linked to the *Ets1* gene in a first backcross from NOD to C57BL/6 mice. These results indicate that allelic variation of *Ets1* did not contribute to variation in NKT cell numbers in these mice. It remains possible that a third factor not linked to the *Ets1* locus controls both ETS1 expression and subsequently NK and NKT cell phenotypes. Candidates for these factors are genes within the two linkage regions identified as controlling NKT cell numbers in mapping studies involving NOD mice: *Nkt1* on chromosome 1 [49, 50] and *Nkt2* on chromosome 2 [50, 51].

Acknowledgments: Alan G. Baxter is supported by an Australian National Health and Medical Research Council (NHMRC) Senior Research Fellowship. This project was funded by the NHMRC. We are grateful to Dr. Luis Esteban for technical advice, Mr. Michael C. Butler for debugging and recompiling Mapmaker/QTL to run on the Pentium 4 and Dr. Vladimir Brusic for helpful discussion.

Conflict of interest statement: The authors declare that they have no conflict of interests.

■ References

1. **Seth A, Ascione R, Fisher RJ, Mavrothalassitit GJ, Bhat NK, Papas TS.** The ets gene family. *Cell Growth Differ* 1992. 3:327-334.
2. **Dwyer J, Li H, Xu D, Liu JP.** Transcriptional regulation of telomerase activity: roles of the the Ets transcription factor family. *Ann N Y Acad Sci* 2007. 1114:36-47.
3. **Bhat NK, Komschlies K, Fujiwara S, Fisher RJ, Mathieson BJ, Gregorio TA, Young HA, Kasik JW, Ozato K and Papas TS.** Expression of ets genes in mouse thymocyte subsets and T cells. *J Immunol* 1989. 1142:672-678.
4. **Barton K, Muthusamy N, Fischer C, Ting CN, Walunas TL, Lanier LL, Leiden JM.** The Ets-1 transcription factor is required for the development of natural killer cells in mice. *Immunity* 1998. 9:555-563.
5. **Muthusamy N, Barton K, Leiden JM.** Defective activation and survival of T cells lacking the Ets-1 transcription factor. *Nature* 1995. 377:639-642.
6. **Eyquem S, Chemin K, Fasseu M, Bories JC.** The Ets-1 transcription factor is required for complete pre-T cell receptor function and allelic exclusion at the T cell receptor beta locus. *Proc Natl Acad Sci U S A* 2004. 101:15712-15717.
7. **Bories JC, Willerford DM, Grevin D, Davidson L, Camus A, Martin P, Stehelin D, Alt FW.** Increased T-cell apoptosis and terminal B-cell differentiation induced by inactivation of the Ets-1 proto-oncogene. *Nature* 1995. 377:635-638.
8. **Wang D, John SA, Clements JL, Percy DH, Barton KP, Garrett-Sinha LA.** Ets-1 deficiency leads to altered B cell differentiation, hyperresponsiveness to TLR9 and autoimmune disease. *Int Immunol* 2005. 17:1179-1191.
9. **Eyquem S, Chemin K, Fasseu M, Chopin M, Sigaux F, Cumano A, Bories JC.** The development of early and mature B cells is impaired in mice deficient for the Ets-1 transcription factor. *Eur J Immunol* 2004. 34:3187-3196.
10. **Roger T, Miconnet I, Schiesser AL, Kai H, Miyake K, Calandra T.** Critical role for Ets, AP-1 and GATA-like transcription factors in regulating mouse Toll-like receptor 4

(Tlr4) gene expression. *Biochem J* 2005. 387(Pt 2):355-365.
11. **Walunas TL, Wang B, Wang CR, Leiden JM.** Cutting edge: the Ets1 transcription factor is required for the development of NK T cells in mice. *J Immunol* 2000. 164:2857-2860.
12. **Koizumi H, Horta MF, Youn BS, Fu KC, Kwon BS, Young JD, Liu CC.** Identification of a killer cell-specific regulatory element of the mouse perforin gene: an Ets-binding site-homologous motif that interacts with Ets-related proteins. *Mol Cell Biol* 1993. 13:6690-6701.
13. **Serreze DV, Choisy-Rossi CM, Grier AE, Holl TM, Chapman HD, Gahagan JR, Osborne MA, Zhang W, King BL, Brown A, et al.** Through regulation of TCR expression levels, an Idd7 region gene(s) interactively contributes to the impaired thymic deletion of autoreactive diabetogenic CD8+ T cells in nonobese diabetic mice. *J Immunol* 2008. 180:3250-3259.
14. **Baxter AG, Mandel TE.** Hemolytic anemia in non-obese diabetic mice. *Eur J Immunol* 1991. 21:2051-2055.
15. **Baxter AG, Horsfall AC, Healey D, Ozegbe P, Day S, Williams DG, Cooke A.** Mycobacteria precipitate an SLE-like syndrome in diabetes-prone NOD mice. *Immunology* 1994. 83:227-231.
16. **Horsfall AC, Howson R, Silveira P, Williams DG, Baxter AG.** Characterization and specificity of B-cell responses in lupus induced by *Mycobacterium bovis* in NOD/Lt mice. *Immunology* 1998. 95:8-17.
17. **Jordan MA, Silveira PA, Shepherd DP, Chu C, Kinder SJ, Chen J, Palmisano LJ, Poulton LD, Baxter AG.** Linkage analysis of systemic lupus erythematosus induced in diabetes-prone nonobese diabetic mice by *Mycobacterium bovis*. *J Immunol* 2000. 165:1673-1684.
18. **Silveira PA, Baxter AG.** The NOD mouse as a model of SLE. *Autoimmunity* 2001. 34:53-64.
19. **Hawke CG, Painter DM, Kirwan PD, Van Driel RR, Baxter AG.** Mycobacteria, an environmental enhancer of lupus nephritis in a mouse model of systemic lupus erythematosus. *Immunology* 2003. 108:70-78.
20. **Poulton LD, Smyth MJ, Hawke CG, Silveira P, Shepherd D, Naidenko OV, Godfrey DI, Baxter AG.** Cytometric and functional analyses of NK and NKT cell deficiencies in NOD mice. *Int Immunol* 2001. 13:887-896.
21. **Baxter AG, Kinder SJ, Hammond KJ, Scollay R, Godfrey DI.** Association between alphabetaTCR+CD4-CD8- T-cell deficiency and IDDM in NOD/Lt mice *Diabetes* 1997. 46:572-582.
22. **Godfrey DI, Kinder SJ, Silvera P, Baxter AG.** Flow cytometric study of T cell development in NOD mice reveals a deficiency in alphabetaTCR+CDR-CD8- thymocytes. *J Autoimmun* 1997. 10:279-285.
23. **Hammond KJ, Poulton LD, Palmisano LJ, Silveira PA, Godfrey DI, Baxter AG.** alpha/beta-T cell receptor (TCR)+CD4-CD8- (NKT) thymocytes prevent insulin-dependent diabetes mellitus in nonobese diabetic (NOD)/Lt mice by the influence of interleukin (IL)-4 and/or IL-10. *J Exp Med* 1998. 187:1047-1056.
24. **Hammond KJ, Pellicci DG, Poulton LD, Naidenko OV, Scalzo AA, Baxter AG, Godfrey DI.** CD1d-restricted NKT cells: an interstrain comparison. *J Immunol* 2001. 167:1164-11673.
25. **Lehuen A, Lantz O, Beaudoin L, Laloux V, Carnaud C, Bendelac A, Bach JF, Monteiro RC.** Overexpression of natural killer T cells protects Valpha14- Jalpha281 transgenic nonobese diabetic mice against diabetes. *J Exp Med* 1998. 188:1831-1839.
26. **Hong S, Wilson MT, Serizawa I, Wu L, Singh N, Naidenko OV, Miura T, Haba T, Scherer DC, Wei J, et al.** The natural killer T-cell ligand alpha-galactosylceramide prevents autoimmune diabetes in non-obese diabetic mice. *Nat Med* 2001. 7:1052-1056.
27. **Sharif S, Arreaza GA, Zucker P, Mi QS, Sondhi J, Naidenko OV, Kronenberg M, Koezuka Y, Delovitch TL, Gombert JM, et al.** Activation of natural killer T cells by alpha-galactosylceramide treatment prevents the onset and recurrence of autoimmune type 1 diabetes. *Nat Med* 2001.7:1057-1062.
28. **Wang B, Geng YB, Wang CR.** CD1-restricted NK T cells protect nonobese diabetic mice from developing diabetes. *J Exp Med* 2001. 194:313-320.
29. **Shi FD, Flodstrom M, Balasa B, Kim SH, Van Gunst K, Strominger JL, Wilson SB, Sarvetnick N.** Germ line deletion of the CD1 locus exacerbates diabetes in the NOD mouse. *Proc Natl Acad Sci U S A* 2001. 98:6777-6782.
30. **Allison J, McClive P, Oxbrow L, Baxter AG, Morahan G, Miller JF.** Genetic requirements for acceleration of diabetes in non-obese diabetic mice expressing interleukin-2 in islet beta-cells. *Eur J Immunol* 1994. 24:2535-2541.
31. **Lander ES, Green P, Abrahamson J, Barlow A, Daly MJ, Lincoln SE, Newberg LA.** MAPMAKER: an interactive computer package for constructing primary genetic linkage maps of experimental and natural populations. *Genomics* 1987. 1:174-181.
32. **Lander E, Kruglyak L.** Genetic dissection of complex traits: guidelines for interpreting and reporting linkage results. *Nat Genet* 1995.11:241-247.
33. **Raouf A, Li V, Kola I, Watson DK, Seth A.** The Ets1 proto-oncogene is upregulated by retinoic acid: characterization of a functional retinoic acid response element in the Ets1 promoter. *Oncogene* 2000. 19:1969-1974.
34. **Jorcyk CL, Garrett LJ, Maroulakou IG, Watson DK, Green JE.** Multiple regulatory regions control the expression of Ets-1 in the developing mouse: vascular expression conferred by intron I. *Cell Mol Biol (Noisy-le-grand)* 1997. 43(2):211-225.
35. **Gilles F, Raes MB, Stehelin D, Vandenbunder B, Fafeur V.** The c-ets-1 proto-oncogene is a new early-response gene differentially regulated by cytokines and growth factors in human fibroblasts. *Exp Cell Res* 1996. 222:370-378.
36. **Wang DY, Yang VC, Chen JK.** Oxidized LDL inhibits vascular endothelial cell morphogenesis in culture. *In Vitro Cell Dev Biol Anim* 1997. 33:248-255.
37. **Prestridge DS.** Predicting pol II promoter sequences using transcription factor binding sites. *J Mol Biol* 1995. 249(5):923-932.
38. **Jorcyk CL, Watson DK, Mavrothalassitis GJ, Papas TS.** The human ETS1 gene: genomic structure, promoter characterization and alternative splicing. *Oncogene* 1991. 6:523-532.
39. **Lionneton F, Lelievre E, Baillat D, Stehelin D, Soncin F.** Characterization and functional analysis of the p42Ets-1 variant of the mouse Ets-1 transcription factor. *Oncogene* 2003. 22:9156-9164.
40. **Moisan J, Grenningloh R, Bettelli E, Oukka M, Ho IC.** Ets-1 is a negative regulator of Th17 differentiation. *J Exp Med* 2007. 204:2825-2835.

41. **Baxter AG, Cooke A.** The genetics of the NOD mouse. *Diabetes Metab Rev* 1995. 11:315-35.
42. **Biros E, Jordan MA, Baxter AG.** Genes mediating environment interactions in type 1 diabetes. *Rev Diabet Stud* 2005. 2:192-207.
43. **Jordan MA, Baxter AG.** The genetics of immunoregulatory T cells. *J Autoimmun* 2008. 31:237-244.
44. **Godfrey DI, Hammond KJ, Poulton LD, Smyth MJ, Baxter AG.** NKT cells: facts, functions and fallacies. *Immunol Today* 2000. 21:573-583.
45. **Porcelli S, Yockey C, Brenner M, Balk S.** Analysis of T cell antigen receptor (TCR) expression by human peripheral blood CD4-8- alpha/beta T cells demonstrates preferential use of several Vbeta genes and an invariant TCR alpha chain. *J Exp Med* 1993. 178:1-16.
46. **Makino S, Kunimoto K, Muraoka Y, Mizushima Y, Katagiri K, Tochino Y.** Breeding of a non-obese, diabetic strain of mice. *Jikken Dobutsu* 1980. 29:1-13.
47. **Watson DK, McWilliams-Smith MJ, Kozak C, Reeves R, Gearhart J, Nunn MF, Nash W, Fowle JR 3rd, Duesberg P, Papas TS, et al.** Conserved chromosomal positions of dual domains of the ets protooncogene in cats, mice, and humans. *Proc Natl Acad Sci U S A* 1986. 83:1792-1796.
48. **Prochazka M, Leiter EH, Serreze DV, Coleman DL.** Three recessive loci required for insulin-dependent diabetes in nonobese diabetic mice. *Science* 1987. 237:286-289.
49. **Jordan MA, Fletcher JM, Pellicci D, Baxter AG.** *Slamf1*, the NKT cell control gene *Nkt1*. *J Immunol* 2007. 178:1618-1627.
50. **Esteban LM, Tsoutsman T, Jordan MA, Roach D, Poulton LD, Brooks A, Naidenko OV, Sidobre S, Godfrey DI, Baxter AG.** Genetic control of NKT cell numbers maps to major diabetes and lupus loci. *J Immunol* 2003. 171:2873-2878.
51. **Fletcher JM, Jordan MA, Snelgrove SL, Slattery RM, Dufour FD, Kyparissoudis K, Besra GS, Godfrey DI, Baxter AG.** Congenic analysis of the NKT cell control gene *Nkt2* implicates the peroxisomal protein Pxmp4. *J Immunol* 2008. 181:3400-3412.

